Evaluation of MSG-derived global radiation estimates for application in a regional crop model

G.J. Roerink [a], J.S. Bojanowski [b], A.J.W. de Wit [a,*], H. Eerens [c], I. Supit [d], O. Leo [b], H.L. Boogaard [a]

[a] Alterra, Wageningen UR, The Netherlands
[b] Monitoring Agricultural Resources Unit, Institute for Environment and Sustainability, Joint Research Centre, European Commission, I-21020 Ispra (VA), Italy
[c] VITO, Boeretang 200, BE-2400 MOL, Belgium
[d] Earth System Science & Climate Change, Wageningen UR, The Netherlands

A B S T R A C T

Crop monitoring systems that rely on agrometeorologic models require estimates of global radiation. These estimates are difficult to obtain due to the limited number of weather stations that measure this variable. In the present study, we validated the global radiation estimates derived from MeteoSat Second Generation (MSG) and evaluated their use in the European Crop Growth Monitoring System (CGMS). A validation with measurements from four CarboEurope flux towers showed that the MSG estimates are accurate and unbiased (standard deviation between 30 and 51 W/m^2). Moreover, a comparison with global radiation estimates from about 300 operational weather stations throughout Europe confirmed that the quality of the MSG product is high and spatially uniform. We also made an intercomparison between the MSG product and the ECMWF (ERA-INTERIM) and CGMS products at 25 km resolution, thus demonstrating that the CGMS and ECMWF products generally underestimate radiation. Nevertheless, the CGMS product showed irregular spatial patterns of local over- and underestimation, while the ECMWF product consistently underestimated. A trend analysis using a seasonal Mann-Kendall test between 2005 and 2009 did not reveal any significant monotonic trends in the MSG radiation estimates, except for 1 location out of 15. Finally, when we applied the WOFOST crop model for maize throughout Europe, the simulated potential total biomass increased due to higher estimates of global radiation made by MSG. In contrast, the water-limited simulated total-biomass generally decreased due to a higher reference evapotranspiration, causing faster depletion of soil moisture and increased water stress.

© 2012 Elsevier B.V. All rights reserved.

1. Introduction

Most agrometeorological systems for regional crop monitoring and yield forecasting use crop growth simulation models that require the input of soil, management and weather data. To model the impact of weather on crop growth, such models typically operate with daily time steps and use daily estimates of four meteorological variables: minimum and maximum temperature, evapotranspiration, total rainfall and global radiation. Most regionally distributed crop models still rely on meteorological variables measured by weather stations to derive gridded versions of these variables, which can then be used as model inputs. This approach has been implemented in the European Crop Growth Monitoring System (CGMS). Since 1994, CGMS has been used for operational crop monitoring and yield forecasting in the European

Union (Boogaard et al., 2002; de Wit et al., 2010; Genovese, 1998; Vossen and Rijks, 1995). It is operated by the MARS unit (Monitoring of Agricultural ResourceS) of the Joint Research Centre (JRC), which is part of the European Commission. The system is also used to study the effects of climate change (Supit et al., 2010a, 2010b).

Of the four main meteorological variables needed for the models, daily global radiation is most difficult to obtain due to the limited number of weather stations that measure this variable. Global radiation is defined here as the total direct solar radiation and diffuse sky radiation received on a horizontal plane at the earth surface. Of the 3050 stations that operationally report data in the CGMS across Europe, only 400 (13%) provide direct measurements of global radiation (Table 1).

Many approaches have been explored to address the problem of limited availability of station observations by deriving global radiation from related variables like sunshine duration through the well-known Angström-Prescott model (Angström, 1924; Prescott, 1940) or temperature (Hargreaves et al., 1985). As part of the MARS project, a methodology was developed by Supit and Van Kappel (1998) that used observation of cloud cover and temperature to

* Corresponding author at: Centre for Geoinformation, Alterra, Wageningen UR, P.O. Box 47, 6700 AA Wageningen, The Netherlands. Tel.: +31 317 481914.
E-mail address: Allard.dewit@wur.nl (A.J.W. de Wit).

Table 1
Overview of data sources for daily global radiation in Europe.

Product	Derived from	Resolution	Coverage	Time series used
CarboEurope	Flux tower measurements	In situ	>20 sites in Europe[a]	Daily, 2008
MetStations	Operationally reporting weather stations	In situ	Selected countries	Daily, 2005–2009
CGMS	Interpolated from weather stations	25 km × 25 km	Europe	Daily, 2008
ERA-INTERIM	ECMWF reanalysis	0.7° × 0.7°	Global	Daily, 2008
LandSAF-DSSF	MeteoSat Second Generation (MSG)	5 km × 5 km	MeteoSat Disk	Daily, 2005–2009
				Dekadal, 2005–2009

[a] Only data for four towers were available for this study (see Table 2).

derive global radiation. Other approaches have been elaborated which often provide better results due to improved calibration or tuning of the specific equations to local conditions (Abraha and Savage, 2008; Diodato and Bellocchi, 2007; Donatelli and Campbell, 1998; Fortin et al., 2008; Hunt et al., 1998; Podestá et al., 2004; Trnka et al., 2005). Other authors have used stochastic methods to cope with the lack of global radiation measurements (Garcia y Garcia et al., 2008; Hansen, 1999). However, the accuracy of all these methods is constrained by the limitations in the observational record of global radiation.

Another problem is that the global radiation estimates at weather stations, whether measured or derived, represent point locations, which must then be interpolated to obtain gridded fields of daily global radiation. To preserve 90% of the spatial variation in global radiation and temperature, Hubbard (1994) showed that weather stations should not be more than 30 km apart. With relatively few stations measuring global radiation, this grid density is hardly ever reached in Europe.

Geostationary satellites provide an alternative means to derive global solar radiation. Being fixed above a given point on the equator, they continuously scan the exposed part of the Earth disk. The resulting data stream has a high temporal frequency – typically one full scan every 15–30 min – and a high spatial resolution of 5–10 km. Consequently, geostationary satellites monitor the daily evolution of the atmospheric conditions at continental scales and with uniform, high resolution measurements. Methods for deriving global radiation from geostationary satellite imagery have existed for over 30 years (Gautier et al., 1980; Tarpley, 1979) and they have been gradually improved and operationalized due to increasing computational power and data availability (Cano et al., 1986; Rigollier et al., 2004; Schulze-Kegel and Heidt, 1996). However, an operational service that produces standardized global radiation products was unavailable.

Following the launch in 2004 of the geostationary MSG satellite (MeteoSat Second Generation), dedicated Satellite EUMETSAT Application Facilities (SAFs) have provided MSG-derived high-level products to a variety of user communities (Trigo et al., 2011). For example, the SAF for Land Surface Analyses (LSA SAF, or more commonly "LandSAF") has distributed global radiation estimates since 2005 with the DSSF product (Downwelling Surface Shortwave radiation Flux). In our study, we aimed to determine the extent to which DSSF could replace the current CGMS as an approach for estimating global radiation.

To ensure completeness, the global radiation estimates provided by the ERA-INTERIM reanalysis of the European Centre for Medium-range Weather Forecasting (ECMWF) were included in our analysis (Berrisford et al., 2009; Dee et al., 2011). The meteorological variables derived from ERA-INTERIM are indeed an alternative source for global radiation estimates that can be used for regional crop modelling. More specifically, the availability of a long and consistent time-series (1989–2011) makes ERA-INTERIM an attractive input source (de Wit et al., 2010).

In our study, we performed six tests: (1) the LandSAF DSSF product was validated at the pixel level using high-quality daily global radiation observations from CarboEurope flux towers; (2) a similar pixel-based comparison was made with the daily measurements of operational weather stations; (3) the global radiation estimates from the CarboEurope flux towers were used to assess the CGMS, ECMWF and DSSF products at the level of a 25 km grid cell; (4) taking the DSSF product as a reference, the spatial patterns of the CGMS and ECMWF products were evaluated and statistically characterized over 15 grid cells distributed across Europe; (5) the temporal consistency of the DSSF product was evaluated, as it might have been affected by incremental upgrades of the algorithms between 2005 and 2009; (6) the impact of the DSSF product on the simulated crop yields was evaluated using the WOFOST crop model in CGMS for the year 2008.

2. Datasets

2.1. CarboEurope flux tower radiation measurements

The CarboEurope Integrated Project (Dolman et al., 2006) aims at understanding and quantifying the European terrestrial carbon balance and the associated uncertainties at local, regional and continental scales. To this end, a network of European partners and flux towers has been established that delivers inputs to the CarboEurope Database. This database offers the scientific community eddy covariance measurements of carbon, water, sensible heat and radiation fluxes, which are performed at various European flux tower sites. The data are quality controlled and standardized. The CarboEurope database is an excellent source of data to validate the MSG-derived DSSF product, because it was not used by LandSAF to calibrate its algorithms. The authors had access to daily measurements taken in 2008 from four CarboEurope flux stations that could be used for this validation. Their locations are shown in Fig. 1, with more details in Table 2.

2.2. Weather stations

The CGMS database contains information from about 3050 pan-European stations that deliver daily weather reports. Out of this total, 400 stations performed direct measurements of global radiation between 2005 and 2009; we extracted these measurements from the database. However, we excluded the data from 100 of these stations because they provided fewer than 365 measurements during this period or because the time series appeared to be inconsistent. Such inconsistencies were apparent from significant changes in the variance of the time series; they were probably due to changes in the measurement devices. Most of the weather stations that conduct global radiation measurements are located in the United Kingdom, the Netherlands, Germany, Italy, Portugal, Turkey and Tunisia (Fig. 1). In general, we assumed that the quality of the global radiation estimates from these stations was more variable than data from the CarboEurope flux towers.

2.3. CGMS gridded global radiation estimates

The CGMS meteorological subsystem is used to obtain quality controlled and gridded meteorological products throughout
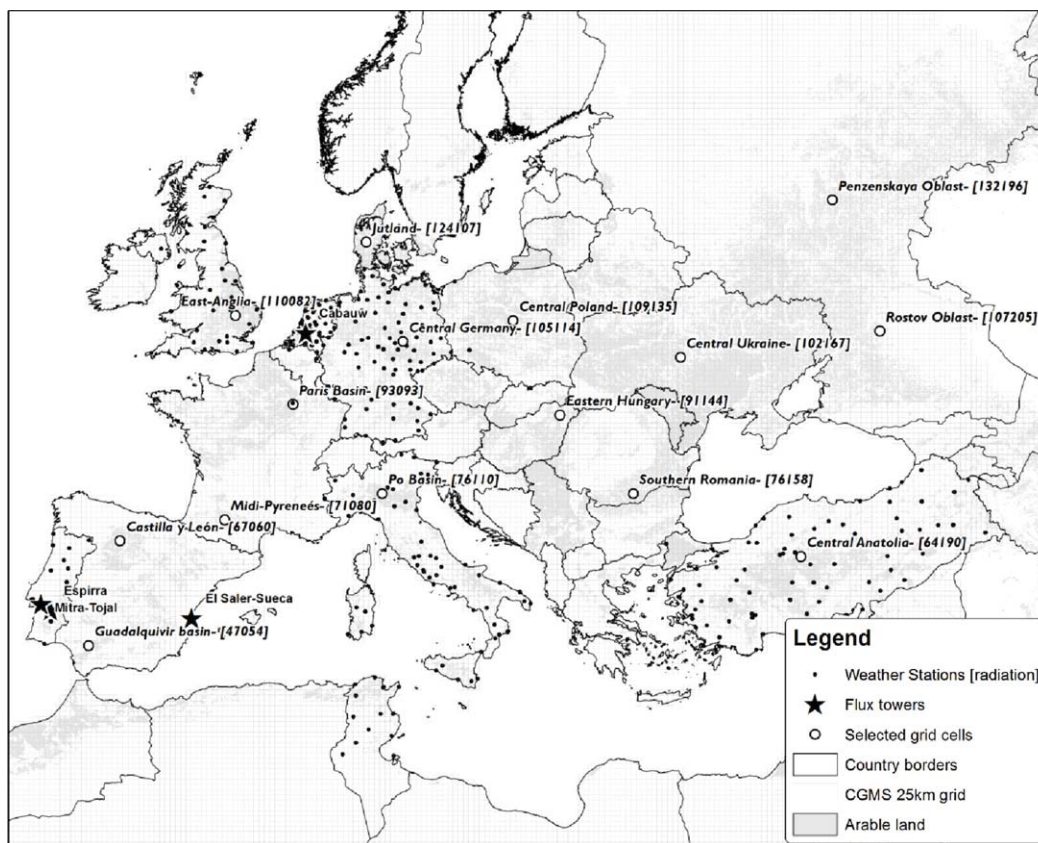
Fig. 1. Overview of the study area in the pan-European continent. In overlay: the country borders, the 25 km CGMS grid, the location of weather stations which directly measure global radiation and the position of the flux towers and selected grid cells. Also the distribution of the arable land is indicated in the background.

Europe for weather monitoring and agro-meteorological modelling purposes. To obtain gridded maps with global radiation, CGMS uses a two-stage approach: (1) global radiation is estimated at station level, and (2) these estimates are interpolated to the 25 km × 25 km grid cells.

To estimate global radiation at the station level, CGMS uses a hierarchical approach that varies with the availability of the following meteorological variables (Supit and Van Kappel, 1998):

1. If observed global radiation is available, this data is used directly. In 2008, this was the case for 400 out of 3050 stations, but for the entire archive (1975–2010), this proportion was much smaller (4%).
2. If sunshine duration data is available, which was the case for 24% of records, global radiation is derived using the Angström equation (Angström, 1924; Prescott, 1940).
3. If cloud cover, minimum and maximum temperature data are available (which is the case for 23% of the records), global radiation is derived with the Supit model.
4. In all the other cases (the remaining 49%), global radiation is derived from the minimum and maximum temperatures using the Hargreaves model (Hargreaves et al., 1985).

The main problem with the application of these radiation models is the quality of the model coefficients. First, the coefficients are derived from stations with observed radiation, and are then interpolated to the others. Studies by Supit (1994) and Supit and Van Kappel (1998) showed no relationship between the coefficients and latitude, even though such relationships are frequently used to estimate the coefficients. Therefore, the same authors identified a set of reference stations that were used to estimate the coefficients in all three models by means of regression techniques. The calibrated model coefficients could then be interpolated to the weather stations without observed global radiation using a simple, distance-weighted average of the three nearest stations.

Global radiation estimates from weather stations are interpolated to the 25 × 25 grid cells of CGMS by calculating the average of up to four suitable stations surrounding the corresponding grid cell. The suitability of the weather stations is based on the 'meteorological distance'. This is a virtual distance that is based not only on the true spatial distance between the cell centre and the weather station, but also on factors such as altitude difference, distance-to-coast and the presence of climate barriers (mountain ridges and water bodies) between the grid cell and the weather station (Beek et al., 1992; Voet et al., 1994).

Table 2
Main characteristics of available CarboEurope flux tower sites.

Station	Code	Longitude	Latitude	Land cover
Espirra, Portugal	PT-Esp	08°01′28.39″W	38°28′35.54″N	Eucalyptus forest
Mitra-Tojal, Potugal	PT-Mi2	08°36′06.48″W	38°38′21.78″N	Grassland
El Saler-Sueca, Spain	ES-Es2	00°18′54.8″W	39°16′31.9″N	Irrigated rice
Cabauw, Netherlands	NL-Ca1	04°55′37.2″E	51°58′15.6″N	Grassland

2.4. ERA-INTERIM radiation product

ERA-INTERIM is the latest ECMWF reanalysis of the global atmosphere during the period 1989 to present and continuing in real time (Berrisford et al., 2009; Dee et al., 2011). The ERA-INTERIM atmospheric model has a spatial resolution of $0.7° \times 0.7°$ and 60 atmospheric layers. Thanks to improved modelling approaches and enhanced inputs, ERA-INTERIM outperforms previous reanalysis data sets such as ERA-40 (ECMWF, 2007).

A two-step procedure has been developed that downscales the $0.7° \times 0.7°$ ERA-INTERIM dataset to the 25 km × 25 km grid cells of the CGMS. First, the 3-hourly ERA-INTERIM values are compiled to daily quantities. Second, an inverse distance weighting is applied to estimate the value of each weather variable at a given CGMS grid cell as the weighted average of the values at the four surrounding ERA-INTERIM grid nodes. More information about the downscaling can be found in de Wit et al. (2010) and (JRC, 2006). To derive the estimates of global radiation for the present study, we applied the procedure to the data from 2008.

2.5. DSSF derived from MSG by LandSAF

Every 15 min, the SEVIRI sensor on the geostationary platform MSG (Meteosat Second Generation) provides a low resolution scan (3 km sub-nadir) of the European and African continents, the Middle East and the eastern tip of Brazil. All the raw data are collected by EUMETSAT (Darmstadt-Germany), pre-processed to a certain extent (calibration, cloud masking, addition of Lon/Lat planes and other operations) and transmitted in near-real time to a network of dedicated SAFs (Satellite Application Facilities). For instance, the NWP SAF deals with numerical weather prediction, the HSAF with hydrological applications and the CM SAF with climatic monitoring.

The Land Surface Analysis group, with headquarters at the Instituto de Meteorologia in Lisbon (Portugal), derives a range of value-added images that are useful for terrestrial monitoring. These images can be divided into three categories: agro-meteorological data (including temperature, solar radiation and evapotranspiration ET), vegetation products (fAPAR, fractional cover, LAI) and fire products (such as radiative power). Some of these derived images retain a high frequency (e.g. LST is generated at 15-min intervals, radiation and ET every 30 min), while others are composited to the daily time step (e.g. the three vegetation products). As summarised in the upper pane of Fig. 2, the data are treated separately for four distinct regions: EURO (Europe), NAFR (northern Africa), SAFR (Africa below the equator) and SAME (South America). The derived images are still in the 'raw' satellite projection, but they can be remapped using the ancillary Lon/Lat-planes generated by EUMETSAT. LandSAF distributes its results in small HDF5-files, which can be acquired via secure FTP (sFTP) or the EUMETcast broadcasting system. Each HDF5-file contains the information for a single one variable (e.g. solar radiation), region (EURO, NAFR, SAFR, SAME) and time step (e.g. 48 files per day for ET, but only one for LAI).

On behalf of the JRC MARS project, VITO (Mol-Belgium) systematically collects the bulk of the MSG-derived information distributed by LSA SAF, in this case all agro-meteorological and vegetation products for the EURO, NAFR and SAFR regions (Fig. 2). The individual data pieces (HDF5) are acquired via sFTP, converted to a more appropriate image format, projected, composited to daily images (if necessary) and then merged together. In this way, separate daily maps are obtained for Europe and Africa. The European maps are assembled from the EURO region and for part of NAFR, and they are expressed in the Lambert Azimuthal Equal-Area projection with a fixed resolution of 5 km (Fig. 2). The African maps include information from NAFR, SAFR and part of EURO. They are mapped using the WGS84 Geographic Lon/Lat system with a
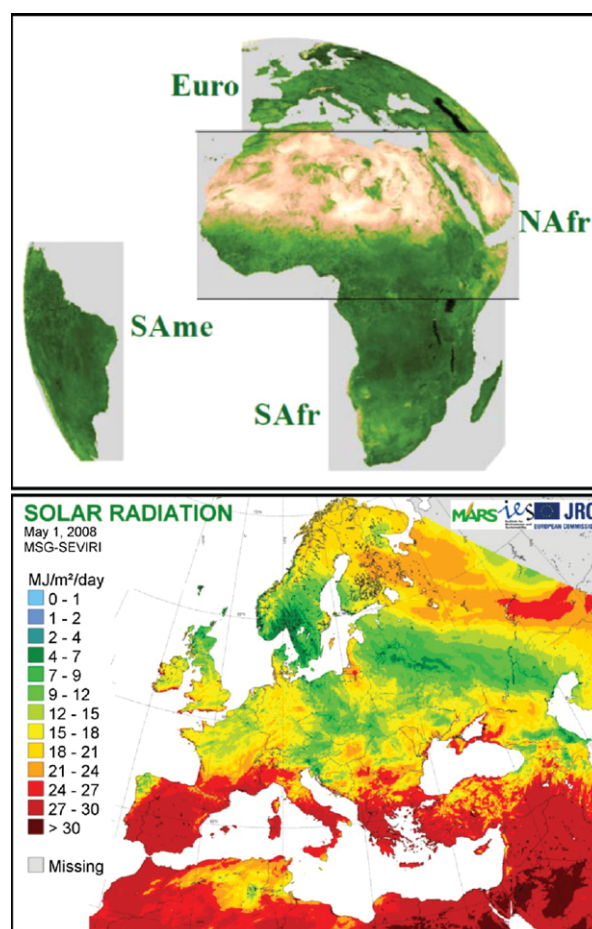
Fig. 2. LandSAF distributes all its MSG-derived products via four separate regions (top pane, figure copied from LandSAF, 2010). The bottom pane shows the daily global radiation (DSSF) for Europe on the first of May, 2008.

resolution of about 4 km. Afterwards, the continental daily scenes are further composited to ten-daily (dekadal) syntheses.

The daily compositing step is needed for high-frequency products such as temperature, ET and solar radiation. A day is defined as the period of 24 h starting at 06:00 h GMT. In the resulting daily images, pixels are labelled as missing if 25% of the actual inputs is lacking, or if they are absent for longer than 4 h. The remaining gaps are filled in by linear interpolation.

In the present study, we focused on the DSSF-product (Downwelling Surface Shortwave radiation Flux) with the solar global radiation estimates. The retrieval algorithm was developed by Météo-France (LandSAF, 2010 – various versions since 2004) and concisely validated by Geiger et al. (2008) using data from seven weather stations across Europe and Africa and some ECMWF forecasts. The daily and dekadal scenes of the entire period 2005–2009 were used. For 2008, the information was lacking for 27 non-contiguous days. We excluded these days from the comparisons, substituting images of preceding or subsequent days in order to run CGMS.

3. Validation and intercomparisons

The methodology can be divided into six steps. First, we validated the LandSAF DSSF product at the pixel level using CarboEurope flux tower measurements. This validation allowed us to quantitatively determine the quality of the DSSF, which we used as a benchmark for further analysis. Second, we evaluated the DSSF product compared to the global radiation measurements from
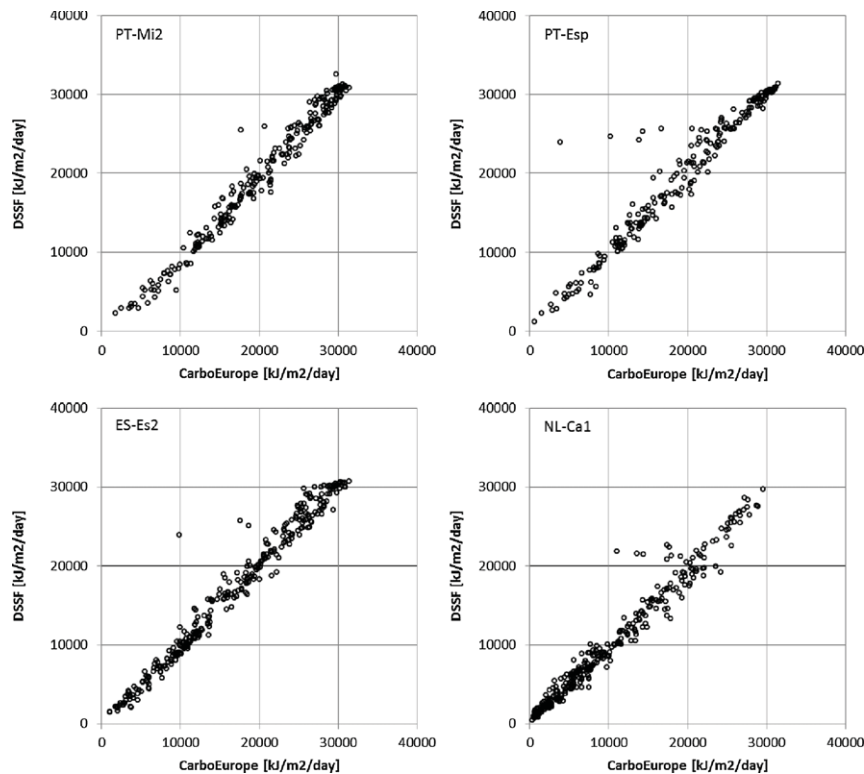
Fig. 3. Validation of LandSAF solar radiation product (DSSF) against in situ measurements (CarboEurope) in Portugal (2×), Spain and the Netherlands.

operational reporting weather stations. Third, to make a comparison between flux tower measurements and the gridded DSSF, CGMS and ECMWF radiation products, we aggregated the DSSF product to the 25 km × 25 km CGMS grid cells. Fourth, taking the DSSF product as a reference, we evaluated the spatial patterns of the CGMS and ECMWF radiation products as well as the statistical differences for 15 selected grid cells that are located in important agricultural areas throughout Europe. Fifth, we analysed the DSSF time-series for trends that could impact the crop yield modelling using the Seasonal Mann-Kendall test (Hirsch and Slack, 1984). Finally, we evaluated the impact on the crop simulations.

3.1. Validation with observed radiation from CarboEurope

The DSSF global radiation product was validated with in situ measurements taken at the four CarboEurope flux tower sites in Portugal (2×), Spain and the Netherlands. The MSG pixels in which the CarboEurope fluxtowers are located were selected, and the time series for 2008 (DSSF global radiation estimates) were retrieved. The CarboEurope flux tower estimates were plotted against the DSSF estimates, and mean error, standard deviation and RMSE were calculated. This allowed us to make a comparison with the accuracy metrics in the DSSF validation report (Geiger et al., 2008; LandSAF, 2008). Note that the daily error estimates in the DSSF validation report were calculated using daytime average values. The global radiation estimates of the DSSF product and the CarboEurope flux towers were therefore recalculated to daytime averages, while taking the astronomical day length into account.

The resulting graphs in Fig. 3 show a high correlation (high R^2 values), and data points are centred on the 1:1 line (regression equations close to $y = x$), which confirms the high quality of the DSSF data. A few outliers can be identified in all four graphs, where the DSSF values are in the range of 25,000 kJ/m²/day

and the CarboEurope values are substantially lower. A closer look at the intra-annual dynamics (Fig. 4) reveals that overall the MeteoSat values follow the in situ measurements closely. However, around 10 April a cluster of daily MeteoSat values with high values – suggesting cloud-free conditions – can be seen, while the in situ measurements shows several downward spikes – suggesting cloud-affected values. Similar patterns around 10 April can be detected for the validation sites in Portugal and Spain. This indicates a problem in the DSSF processing chain.

The error statistics in Table 3 show that the daily global radiation estimates of the DSSF product are essentially unbiased, with a standard deviation between 31 and 51 W/m². These numbers are in the same range as the results presented in the DSSF product validation guide, where standard deviations for daily products between 20 and 44 W/m² are reported (Geiger et al., 2008; LandSAF, 2008).
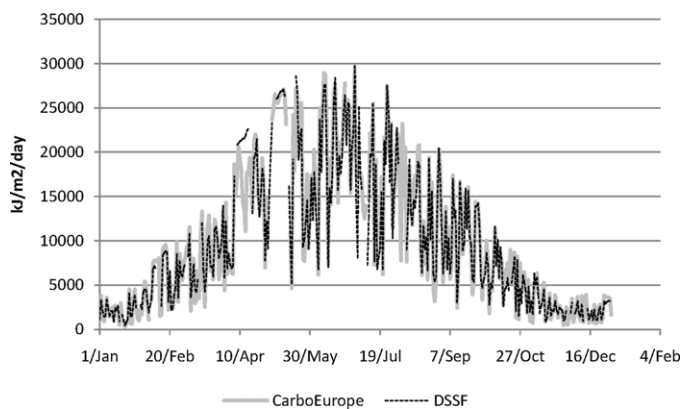
Fig. 4. Global radiation at Cabauw flux station (Netherlands) over 2008 derived from in situ measurements (CarboEurope) and the DSSF product.

Table 3
Error statistics derived from the comparison between daily global radiation observed in 2008 at selected CarboEurope flux towers and the DSSF product.

Flux tower		Mean error (DSSF – CarboEurope)		Standard deviation of errors		RMSE	
ID	Annual mean (kJ/m²/day)	W/m²	kJ/m²/day	W/m²	kJ/m²/day	W/m²	kJ/m²/day
ES-Es2	16,685	0.30	159.07	43.80	1489.00	43.67	1495.16
PT-Mi2	17,356	−11.49	−404.59	31.23	1372.61	33.22	1428.21
PT-Esp	16,802	9.26	469.80	51.13	2356.92	51.84	2397.88
NL-Ca1	10,152	−2.32	−129.53	30.97	1469.44	31.01	1472.88

3.2. Comparison with observed radiation from operational weather stations

We selected the MSG pixels in which the weather stations were located and extracted the daily DSSF radiation estimates for those pixels. Our analysis focussed particularly on the spatial and temporal variability of the differences between DSSF radiation and radiation directly measured at weather stations.

Fig. 5 shows the spatial distribution of the RMSE for the selected stations across Europe that reported radiation measurements. The results indicate that there are many stations with RMSE values in the same order of magnitude (or even lower) as the CarboEurope flux towers, particularly in the United Kingdom, the Netherlands and Germany. Weather stations with RMSE values lower than 2000 kJ/m²/day can be found throughout Europe, indicating that the quality of the LandSAF global radiation estimates are probably quite uniform across Europe. In general, a 'country effect' (i.e. different ranges of RMSE values between different countries) is apparent, which is probably due to different measurement equipment and procedures. In addition, higher RMSE values can be expected at lower latitudes, simply due to increasing global radiation values at these latitudes.

We then summarized the mean error (ME) and the root mean squared error (RMSE) across all stations as box plots (Fig. 6), which demonstrated that 50% of the stations have a mean error (ME) between −180.6 and 1012.9 kJ/m²/day and an RMSE between 1338.8 and 2587.8 kJ/m²/day. This is in the same order of magnitude as the CarboEurope flux towers. However, the summarized mean error includes a group of stations with a large positive mean error, where the DSSF radiation is higher than the radiation observed at the weather stations. Similarly, this group of stations can be identified in the RMSE box plot as having large RMSE. Given the results from the validation with the CarboEurope flux towers and the spatial patterns of the station RMSE, it is likely that these large error values are not caused by inaccuracy in the DSSF-estimated radiation, but by systematic offsets in the radiation estimates from these operational weather stations.

Finally, to identify how the differences between MSG-derived radiation and measured at weather stations change in time, we performed regression analysis for each day separately, taking as dependent variables the direct measurements from all the weather stations and as independent variables the corresponding DSSF values. In this way, the temporal evolution of coefficient of determination and regression coefficients can be shown. The results (Fig. 7)
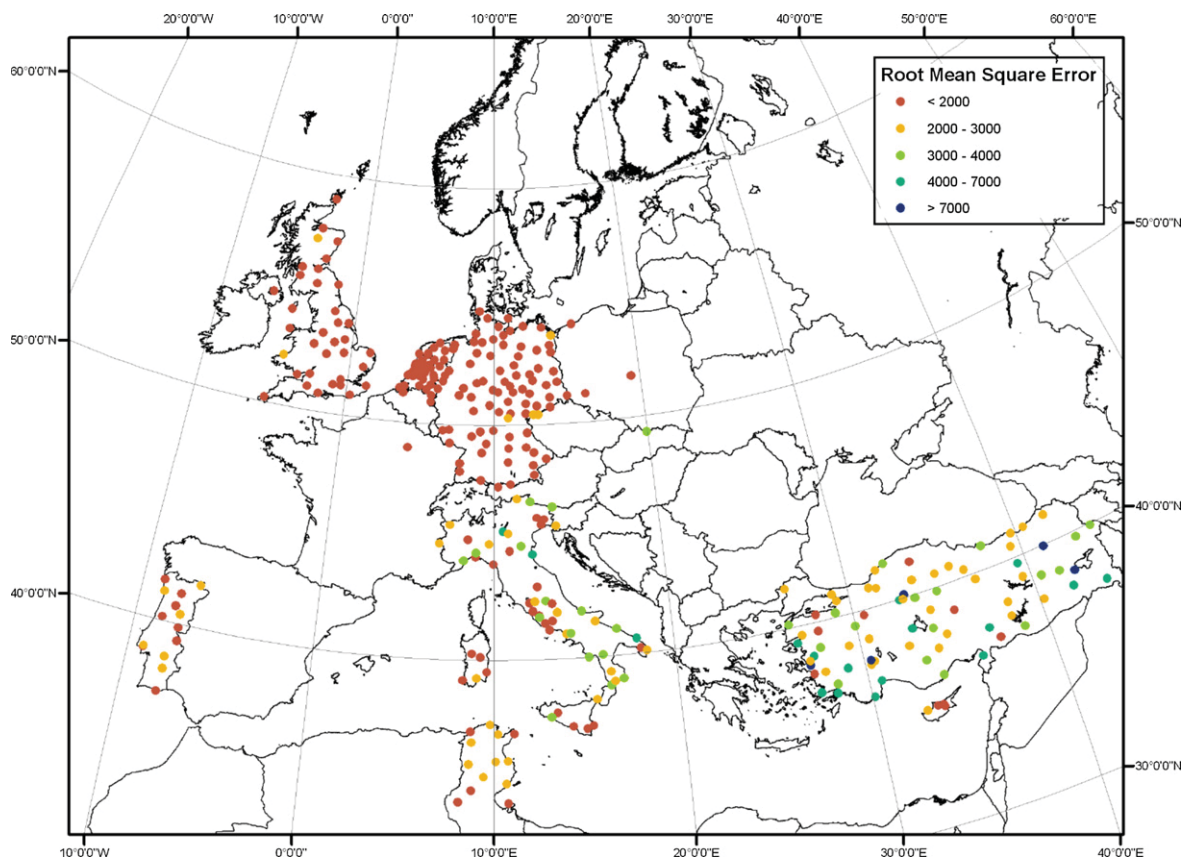
Fig. 5. Spatial distribution of RMSE between observed radiation at operational weather stations and DSSF estimated radiation (kJ/m²/day) over the period 2005–2009.
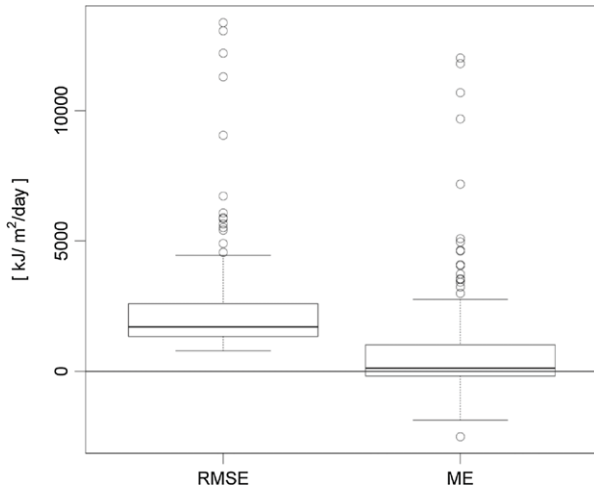
Fig. 6. Boxplot of mean error (ME) and root mean squared error (RMSE) between observed radiation at operational weather stations and DSSF estimated radiation over the period 2005–2009. Mean error calculated as: [DSSF radiation] − [radiation at operational weather stations]. Box indicating the first quartile, median value and third quartile. Whiskers positioned at 1.5 times the inter-quartile range. Circles indicating individual observations beyond the 1.5 interquartile range.

show that R^2, slope, intercept and RMSE all have an annual cycle. The coefficient of determination varied more in 2005 and 2006, but in 2007 and 2008 it had the same behaviour. There were clear minimums in the summer seasons, when R^2 dropped to 0.5–0.7, while outside summer season it remained stable at around 0.8. Slope

(a) tended to approach 1 during the winter season, but dropped to around 0.8 during the summer. This indicates that the DSSF radiation estimates are systematically higher than the station measurements during high radiation levels in the summer. The fact that the intercept (b) is near 0 during the winter, and then increases to around 5000 kJ/m^2/day, confirms that the regression line becomes 'tilted' during the summer. Finally, RMSE also has a strong seasonal character, with the highest values during summer, illustrating the increasing deviations between the radiation estimates during the summer.

3.3. Validation and intercomparison of DSSF, CGMS and ECMWF products

First, we carried out a qualitative evaluation of the global radiation estimates of the CGMS, ECMWF and DSSF products at the 25 km grid level by making a direct comparison with the flux tower measurements, which are assumed to be the absolute reference (Table 4). For the DSSF product, Table 5 also includes the pixel level error statistics (similar to Table 3), thus demonstrating the effect of aggregating to a 25 km grid.

The results indicate that averaging the DSSF 5 km pixels to a 25 km grid has little effect on the error statistics relative to the CarboEurope flux towers. The bias decreases for two stations (ES-Es2, PT-Esp), increases for one station (PT-Mi2) and does not change for one station (NL-Ca1). Standard deviation tends to increase slightly for three out of four stations. Bias for the DSSF-25 km product varies between −491 and 441 kJ/m^2/day, which corresponds with −2.8% and 2.6% of the DSSF annual mean value. For the CGMS product, the bias varies between −3506 and 1295 kJ/m^2/day (−21% to 7.7% of annual mean). The standard deviation also shows a
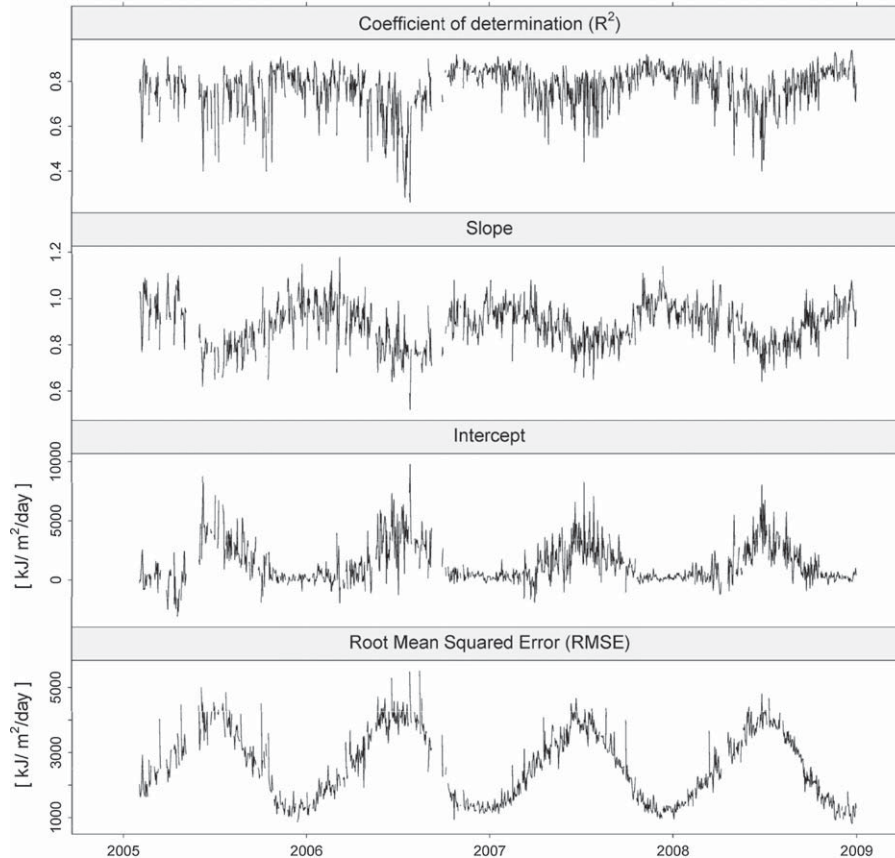
Fig. 7. Temporal evolution of the coefficient of determination (R^2), slope, intercept and root mean squared error (RMSE) derived from linear regression results carried out separately for each day based on all stations' measurements (DSSF estimates as independent and operational radiation estimates as dependent variables).

Table 4
Error statistics from the differences between daily global radiation observed in 2008 at selected CarboEurope flux towers and all radiation products (product-CarboEurope). All values in kJ/m^2/day.

ID	Annual	DSSF 5 km		DSSF 25 km		CGMS		ECMWF	
	Mean	Mean	St Dev	Mean	St Dev	Mean	St Dev	Mean	St Dev
ES-Es2	16,685	159.1	1489.0	−38.4	1534.2	−3506.7	4142.1	−1039.3	2959.5
PT-Mi2	17,356	−404.6	1372.6	−491.4	1427.5	928.9	1550.9	−2264.9	2470.0
PT-Esp	16,802	469.8	2356.9	441.8	2322.2	1295.2	2065.9	−1025.3	2793.4
NL-Ca1	10,152	−129.5	1469.4	−129.9	1480.3	−292.9	1420.6	−395.9	2561.3

large variation between the flux towers, ranging from 4142 to 1420 kJ/m^2/day. Finally, the ECMWF product showed a consistent negative bias (underestimation of global radiation), ranging from −2264 to −396 kJ/m^2/day, and a fairly constant standard deviation, ranging from 2470 to 2959.5 kJ/m^2/day.

Next, for the ECMWF, DSSF and CGMS products, we calculated the annual average global radiation 2008 and plotted this on maps to show systematic spatial differences between the products. The annual patterns of the CGMS product reflect the interpolation method (which is sometimes coarse), while the ECMWF and DSSF images have much smoother spatial patterns (Fig. 8). Strongly deviating patterns between the CGMS and DSSF annual radiation are clearly visible in the Iberian Peninsula, the Maghreb, Egypt, Turkey, Greece, Bulgaria and the Balkans. The spatial patterns of the ECMWF and DSSF images largely resemble each other. The ECMWF values, and to a lesser extent the CGMS values, are systematically lower than the DSSF values.

Fig. 8 illustrates the differences between the annual average radiation of the ECMWF and CGMS products compared to the DSSF product (taking the DSSF as a reference). The ECMWF radiation product generally provided lower global radiation estimates in Europe. For 66% (19%) of the grid cells, the values were within 10% (5%) of the DSSF annual average global radiation. The differences between CGMS and DSSF show a mixed pattern of local underestimation and overestimation of global solar radiation, with more extreme differences in Spain, Algeria, Bulgaria, Greece, Turkey, Egypt and Ukraine/Belarus. For 62% (37%) of the grid cells, the values of the CGMS product are within 10% (5%) of the DSSF annual average global radiation.

Finally, we determined the annual average daily values and daily differences for the three daily global radiation products at 25 km × 25 km for 15 selected grid cells (Table 5) for each day in 2008. This confirms that CGMS and ECMWF generally provide lower

solar radiation estimates than DSSF. However, the error statistics of the ECMWF product (ECMWF − DSSF) are fairly consistent between sites, with a mean error (ME) between −1.2% and −11.8%, a standard deviation (STDEV) between 12.0% and 30.5%, and a RMSE between 17.1% and 30.4%. In contrast, the error statistics of the CGMS product (CGMS − DSSF) show larger differences between sites particularly for the mean error (−30.7% to 7.3%) and to a lesser extent for standard deviation and RMSE (12.1–31.9% for STDEV and 12.1–37.4% for RMSE).

3.4. Trend analysis of DSSF data

During DSSF product generation, several improvements have been implemented in the processing chain, leading to improved DSSF products. However, these improved processing algorithms have not been applied to the MSG archive, which may therefore lead to systematic differences in the DSSF product time-series. This can be problematic because crop yield forecasting relies strongly on the analysis of historical time-series. Therefore, any disruption or trend in the time-series caused by DSSF product upgrades could negatively affect the analysis of historic time-series of simulated and reported yields.

To evaluate the existence of trends in the DSSF product, we analysed the dekadal radiation product between 2005 and 2009. Trends in the dataset were analysed with the seasonal Kendall test, which applies the Mann-Kendall test to individual seasons (in our case dekads) through the year (Hirsch and Slack, 1984). It subsequently combines the results from the tests for individual seasons into an overall test which determines if the dependent (Y) value changes in a consistent direction over time (a monotonic trend). The Kendall test was applied to the 15 selected grid cells for the entire period (2005–2009).

Table 5
Statistical analysis of global radiation data (2008) from CGMS, DSSF and ECMWF over 15 grid cells in Europe.

Average global radiation per day (kJ/m^2/day)			Average global radiation differences per day (kJ/m^2/day and %)											
CGMS	DSSF	ECMWF	CGMS − DSSF						ECMWF − DSSF						
			ME		STDEV		RMSE		ME		STDEV		RMSE	
18,023	18,304	17,094	−281	−2%	2204	12%	2219	12%	−1210	−7%	2887	16%	3126	17%
11,870	17,141	15,617	−5271	−31%	3653	21%	6410	37%	−1524	−9%	3035	18%	3392	20%
14,860	16,146	14,236	−1286	−8%	2473	15%	2785	17%	−1910	−12%	2908	18%	3476	22%
12,282	12,940	12,780	−658	−5%	3097	24%	3162	24%	−159	−1%	3666	28%	3664	28%
11,674	14,166	13,185	−2492	−18%	3242	23%	4086	29%	−981	−7%	3779	27%	3899	28%
14,537	14,951	13,708	−414	−3%	2583	17%	2612	17%	−1242	−8%	3281	22%	3504	23%
10,285	12,830	12,087	−2545	−20%	3538	28%	4355	34%	−743	−6%	3246	25%	3325	26%
9854	11,078	10,781	−1223	−11%	2788	25%	3041	27%	−297	−3%	3070	28%	3080	28%
11,559	11,811	11,036	−253	−2%	3673	31%	3676	31%	−775	−7%	3171	27%	3260	28%
10,686	10,756	10,518	−71	−1%	2635	24%	2632	24%	−238	−2%	3264	30%	3268	30%
11,921	12,876	12,236	−955	−7%	3112	24%	3251	25%	−641	−5%	3211	25%	3270	25%
9652	11,018	10,237	−1366	−12%	2734	25%	3053	28%	−781	−7%	3227	29%	3316	30%
9367	9833	9624	−466	−5%	2308	23%	2352	24%	−209	−2%	2754	28%	2758	28%
10,605	9883	9648	722	7%	2314	23%	2421	24%	−235	−2%	2367	24%	2375	24%
11,114	11,091	9981	23	0%	2660	24%	2656	24%	−1110	−10%	2674	24%	2892	26%
Minimum:			−5271	−31%	2204	12%	2219	12%	−1910	−12%	2367	16%	2375	17%
Maximum:			722	7%	3673	31%	6410	37%	−159	−1%	3779	30%	3899	30%
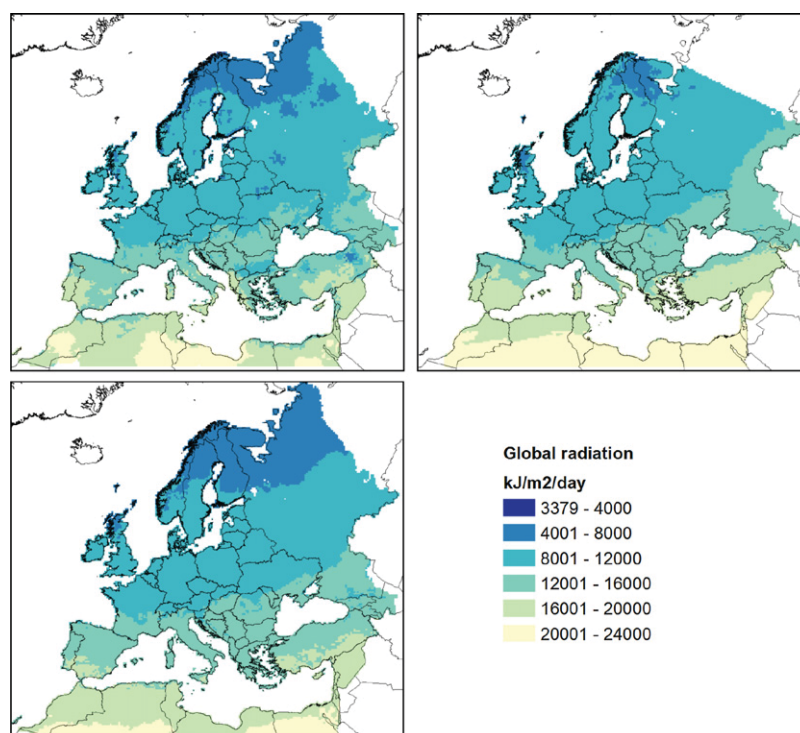
Fig. 8. 2008 annual average global radiation estimated by CGMS (upper-left), DSSF (upper-right) and ECMWF (lower-left).

The results from the Seasonal Kendall test (Table 6) indicate that only one grid cell (76158) showed a significant monotonic trend in the radiation values over the period 2005–2009 ($p < 0.05$). Also, 8 grid cells showed a positive Kendall Tau value and 7 grid cells a negative one, indicating that the direction of the non-significant trends is equally distributed across negative/positive trends.

3.5. Impact on simulated crop yields

We used the Crop Growth Monitoring System with the CGMS and DSSF global radiation datasets as input for 2008. Other weather variables (temperature, humidity, rainfall, windspeed) were interpolated from weather stations. The setup of the system with regard to crop calendars, cultivars and soil types was equivalent to that described in (de Wit et al., 2010). Grain maize was selected as an example, because we expected that the impact of differences in the radiation level between the two products could be more pronounced for a summer crop.

Table 6
Kendall Tau and p values derived from the seasonal Kendall test on the decadal DSSF global radiation estimates for each grid cell over the period 2005–2009.

Grid	Location	Kendall Tau	p-Value
47054	Guadalquivir basin	−0.021	0.8164
64190	Castilla y León	0.075	0.3296
67060	Midi-Pyreneés	−0.014	0.8892
71080	East-Anglia	−0.11	0.15
76110	Paris Basin	−0.027	0.7452
76158	Jutland	0.164	0.0291
91144	Po Basin	0.027	0.7452
93093	Central Germany	0.014	0.8892
102167	Central Poland	0.062	0.43
105114	Eastern Hungary	−0.041	0.6096
107205	Southern Romania	0.099	0.1932
109135	Central Ukraine	−0.089	0.2458
110082	Central Anatolia	−0.027	0.752
124107	Penzenskaya Obl.	0.014	0.8892
132196	Rostov Oblast	0.034	0.6761

Two system outputs were selected: (1) the potential total biomass production at the end of the growing season, which depends only on temperature, radiation and crop management, and (2) the water-limited total biomass production at the end of the growing season, whereby water-limitation and transpiration also play a role. Water availability is determined only by initial water availability (assumed to be field capacity) and rainfall. The influence of irrigation or groundwater is currently not taken into account. The potential and water-limited biomass production of maize in 2008 is presented in Figs. 10 and 11. Northern Europe is not included, because climatic conditions there are not suitable for maize cultivation.

The potential biomass production of maize is directly related to the total amount of solar radiation intercepted by the crop canopy. Consequently, the differences in biomass production between default CGMS and CGMS with DSSF global radiation as input are also directly linked to the differences between both radiation sources. Fig. 10 shows the same pattern as Fig. 9; in South-Spain, North-France, Turkey, Greece, Bulgaria and Poland/Belarus/Ukraine the default simulated biomass is again lower compared to the DSSF simulated biomass, due to lower estimates of global radiation by default CGMS. A slight overestimation is present in Portugal, parts of Britain, the French Alps and the French Central Plateau.

The CGMS water-limited biomass simulation results show a strong North-South gradient (Fig. 11). This is caused by the decreasing precipitation rates and increasing evapotranspiration rates towards the South of Europe, leading to greater yield losses as a result of water limitation. In general, the differences between the water-limited simulated biomasses of the two global radiation sources are smaller than the differences in potential production. Crop growth is obviously water limited, so the differences in solar radiation input have limited effect.

In the potential production case, most grids have negative differences (DSSF biomass larger than default biomass), but in the water-limited production case the situation is generally reversed,
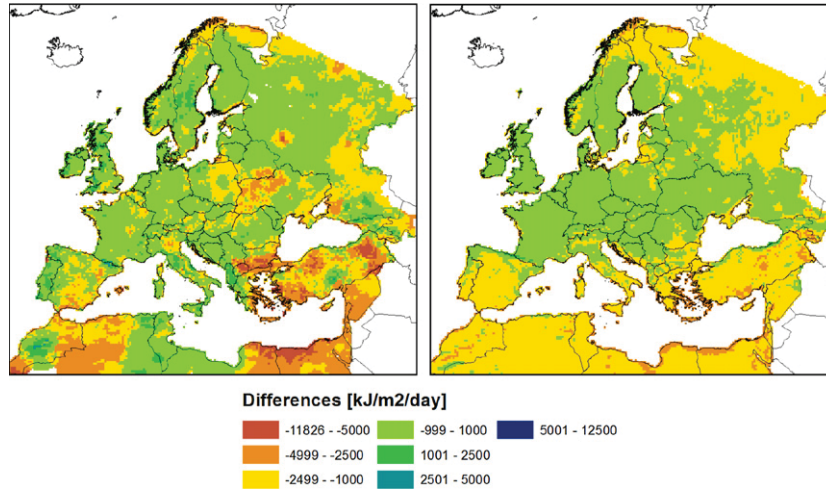
Fig. 9. 2008 Differences between annual average global radiation estimates: CGMS minus DSSF (left) and ECMWF minus DSSF (right).

and many grid cells show positive differences (DSSF biomass lower than default biomass). This effect is caused by the estimated reference evapotranspiration, which also reacts to differences in radiation inputs. In the case of DSSF inputs, the reference evapotranspiration levels are generally higher, causing faster depletion of the available soil moisture. Consequently, the crop model simulates increased water-stress on crop growth, leading to lower crop biomass.
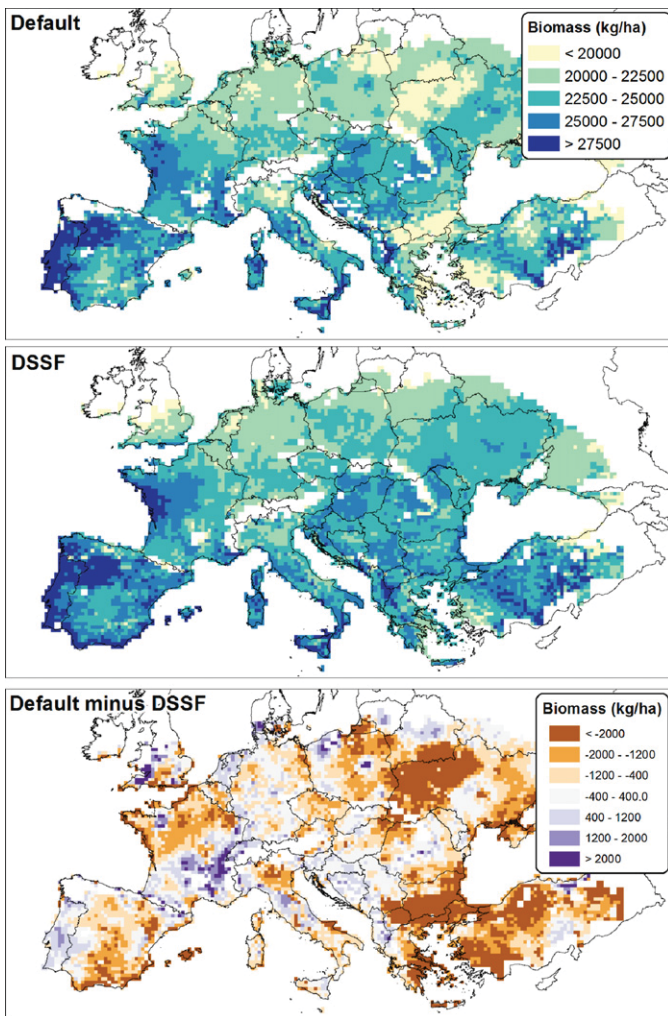
Fig. 10. Potential total above-ground biomass of maize as calculated by CGMS (25 km grid) using standard CGMS global radiation (above), DSSF global radiation (middle) and the differences between the 2 outputs (below).
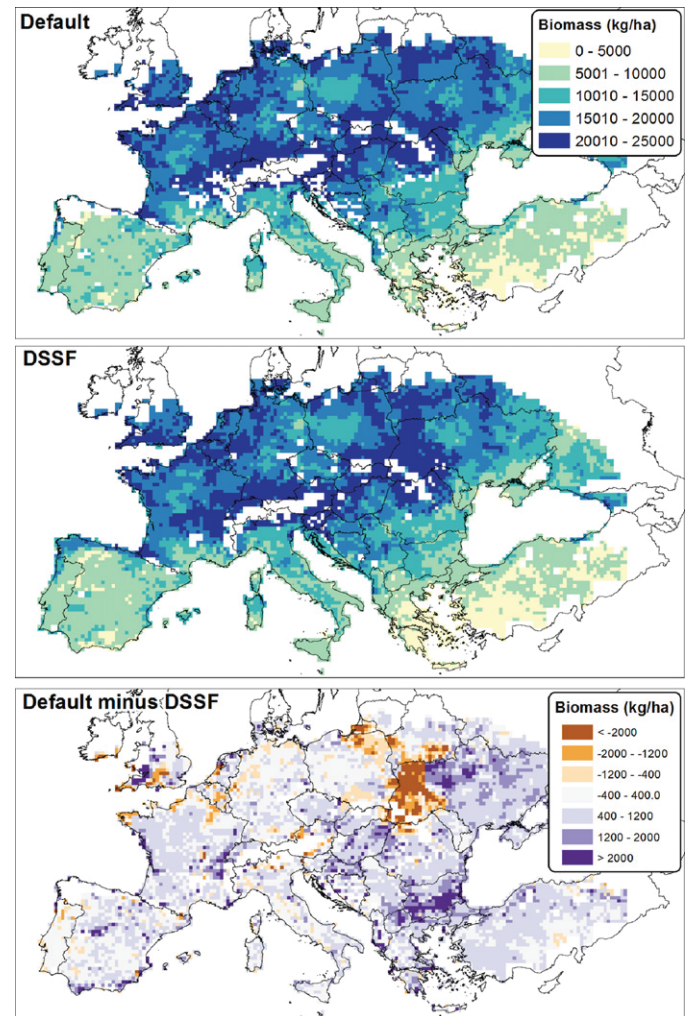
Fig. 11. Water-limited total above-ground biomass of maize in 2008 as calculated by CGMS standard (above) CGMS with DSSF global radiation as input (middle) and the differences (below).

An extreme example of this effect can be seen in southern Bulgaria. Under potential production conditions, CGMS with DSSF inputs simulated much higher biomass values (negative difference lower than −2000 kg/ha), while under water-limited conditions, the effect was reversed due to increased drought stress. Moreover, the CGMS with DSSF inputs simulated much lower biomass values (positive difference greater than 2000 kg/ha).

In western Ukraine, another striking pattern is visible: abrupt spatial changes between the simulated biomass values of CGMS with default and DSSF inputs. Analysis of two neighbouring grid cells with large differences indicates that this is caused by a large difference in rainfall pattern. In the region with negative differences, some large rainfall events in July increased soil moisture levels above the critical level, thus allowing the simulations with both default and DSSF inputs to continue without much water stress. In this case, the higher DSSF radiation inputs led to larger simulated biomass values.

In the region with positive differences, the July rainfall events were lacking, causing the simulations with DSSF inputs to deplete the soil moisture must faster than the default simulations due to the larger reference evapotranspiration. Consequently, the simulations with DSSF inputs indicated much more water stress, leading to a difference in simulated biomass values of around 4500 kg/ha. In contrast, the default simulated biomass values between the two grid cells showed a much smaller difference of about 1000 kg/ha. This clearly illustrates the non-linear impact of differences in radiation inputs that sometimes occurs.

4. Discussion

The validation with CarboEurope flux tower measurements showed that the DSSF solar radiation product is high quality. The coefficients of determination (R^2) between the MSG DSSF radiation product and the CarboEurope measurements are always higher than 0.9, and the relationships are close to the ideal $y = x$ equation. Moreover, the error statistics derived from the four CarboEurope stations are in agreement with the statistics reported in the DSSF validation report.

The comparison with radiation measurements from operational reporting weather stations indicates that similar error statistics can be obtained for a considerable number of stations relative to the CarboEurope stations. Given that these stations are distributed throughout Europe, we can argue that the quality of the DSSF product is probably quite uniform throughout Europe. The maps and box plots indicate that one group of stations showed much larger differences (ME and RMSE), which is probably not related to spatial differences in the DSSF product, but rather to the quality of the measurements at these operational weather stations due to different measurement equipment and procedures. This assumption is supported by the fact that out of 400 selected stations, 100 were excluded beforehand because they showed inconsistent measurements. Finally, the temporal analysis showed that the differences in global radiation between DSSF and operational weather stations are seasonal, with the largest deviations during the summer period.

Regarding the analysis using operational weather stations, one qualification is that no radiation measurements were available at high latitudes (>55N), where MSG has a very large viewing angle that could deteriorate the DSSF product. However, even at high latitudes the DSSF product did not show large differences with ECMWF model estimates of global radiation.

The validation of the three 25-km gridded solar radiation products (DSSF-25 km, ECMWF, CGMS) also indicates that the DSSF radiation estimates, when aggregated to 25-km resolution, are still close to the flux tower estimates. The CGMS radiation estimates both underestimated and overestimated the flux tower estimates,

while the ECMWF (ERA-INTERIM) product systematically underestimated radiation. The latter is in contrast with the findings of Szczypta et al. (2011), who reported that ERA-INTERIM overestimates observed global radiation.

The intercomparison of the three gridded solar radiation products (DSSF, ECMWF, CGMS) indicates that the CGMS and ECMWF products provide lower global radiation estimates compared to DSSF. Moreover, the CGMS gridded global radiation values result in irregular spatial patterns or artefacts, not only due to the interpolation procedures, but also because the CGMS values are a mixture of measured radiation and radiation values based on either sunshine duration, cloud cover and temperature or temperature only. Irregular patterns could be caused by the different origin of radiation values between grid cells. In cases where neighbouring grid cells are based on different methods (e.g. temperature vs. sunshine duration), this could cause a sharp change that cannot be attributed to the interpolation method itself. In contrast, the differences between the DSSF and ECMWF products are consistent across the various locations tested.

A trend analysis was performed on the basis of 163 decades, between 2005 and 2009, at 15 locations throughout Europe. The seasonal Kendall test indicated that no significant monotonic trends could be found, except for one location. Moreover, the directions of non-significant trends were balanced between positive and negative. Nevertheless, EUMETSAT has recently started reprocessing of the MSG archive older than June 2008, which may eliminate effects caused by algorithm upgrades (EUMETSAT, 2011).

Finally, the impact of differences in global radiation estimates between the CGMS and DSSF products on simulated potential crop production is considerable and appears to be directly related to differences in solar radiation; higher DSSF estimates of global radiation resulted in increased potential crop production. In case of water-limited crop production, the differences were generally smaller, but the overall pattern was reversed: default CGMS with higher crop production due to lower estimates of reference evapotranspiration and lower levels of crop water stress. Locally, the impact on the water-limited simulation results can be highly non-linear, depending on the rainfall pattern and soil properties.

5. Conclusions

The overall objective of this study was to determine whether the MSG-derived DSSF product could replace the current approach for estimating global radiation throughout Europe in the MARS crop yield forecasting system.

In general, it can be concluded that the LandSAF DSSF global radiation product is a major improvement over the current approach for deriving global radiation implemented in CGMS, both in terms of absolute values and spatial patterns. Nevertheless, operational implementation of the LandSAF DSSF product in the CGMS production chain is not yet possible because the time-series are too short. The CGMS crop yield forecasting system relies on regression between time-series of historic simulated and reported crop yields at the regional level, which requires a consistent time-series of 10–15 years. Combined use of the default radiation estimates (pre-2005) and the DSSF estimates (post-2005) would cause systematic changes in the simulated biomass values, which would distort the historic analysis. Moreover, to evaluate abnormal weather events relative to climate, a period of 30 years is preferred.

A first step in improving CGMS could be taken by deriving global radiation estimates from the DSSF product for each weather station in CGMS during the available MSG time-series. The DSSF radiation estimates could then provide station-specific calibration for the global radiation models included in CGMS (e.g. Angström, Supit, Hargreaves). This has the advantage of eliminating the

need for reference stations and avoiding the sometimes coarse extrapolation of model parameters to surrounding stations (see Section 2.3). In a second step, data from MeteoSat First Generation could be used to replace the historic archive. Such data have recently been back-processed in order to provide a 25-year record of global radiation estimates (Posselt et al., 2010). This could be used to provide the archive needed by CGMS.

Acknowledgements

References

Abraha, M.G., Savage, M.J., 2008. Comparison of estimates of daily solar radiation from air temperature range for application in crop simulations. Agricultural and Forest Meteorology 148 (3), 401–416.

Angström, A., 1924. Solar and terrestrial radiation. Quarterly Journal of the Royal Meteorological Society 50, 121–125.

Beek, E.G., Stein, A., Jansen, L.L.F., 1992. Spatial variability and interpolation of daily precipitation amount. Stochastic Hydrology and Hydra 6, 304–320.

Berrisford, P., Dee, D., Fielding, K., Fuentes, M., Kallberg, P., Kobayashi, S., Uppala, S., 2009. The ERA-Interim Archive. ERA Report Series. ECMWF, Shinfield Park, Reading, 16 pp.

Boogaard, H.L., Eerens, H., Supit, I., Diepen, C.A.v., Piccard, I., Kempeneers, P., 2002. Description of the MARS Crop Yield Forecasting System (MCYFS), Joint Research Centre, Study contract number 19226-2002-02-F1FED ISP NL.

Cano, D., Monget, J.M., Albuisson, M., Guillard, H., Regas, N., Wald, L., 1986. A method for the determination of the global solar radiation from meteorological satellite data. Solar Energy 37 (1), 31–39.

de Wit, A.J.W., Baruth, B., Boogaard, H.L., Diepen, C.A.v., Kraalingen, D.v., Micale, F., te Roller, J., Supit, I., van de Wijngaart, R., 2010. Using ERA-INTERIM for regional crop yield forecasting in Europe. Climate Research.

Dee, D.P., Uppala, S.M., Simmons, A.J., Berrisford, P., Poli, P., Kobayashi, S., Andrae, U., Balmaseda, M.A., Balsamo, G., Bauer, P., Bechtold, P., Beljaars, A.C.M., van de Berg, L., Bidlot, J., Bormann, N., Delsol, C., Dragani, R., Fuentes, M., Geer, A.J., Haimberger, L., Healy, S.B., Hersbach, H., Hólm, E.V., Isaksen, L., Kållberg, P., Köhler, M., Matricardi, M., McNally, A.P., Monge-Sanz, B.M., Morcrette, J.J., Park, B.K., Peubey, C., de Rosnay, P., Tavolato, C., Thépaut, J.N., Vitart, F., 2011. The ERA-Interim reanalysis: configuration and performance of the data assimilation system. Quarterly Journal of the Royal Meteorological Society 137 (656), 553–597.

Diodato, N., Bellocchi, G., 2007. Modelling solar radiation over complex terrains using monthly climatological data. Agricultural and Forest Meteorology 144 (1–2), 111–126.

Dolman, A.J., Noilhan, J., Durand, P., Sarrat, C., Brut, A., Piguet, B., Butet, A., Jarosz, N., Brunet, Y., Loustau, D., Lamaud, E., Tolk, L., Ronda, R., Miglietta, M., Gioli, B., Magliulo, V., Esposito, M., Gerbig, C., Körner, S., Glademard, P., Ramonet, M., Cias, P., Neininger, B., Hutjes, R.W.A., Elbers, J.A., Macatangay, R., Schrems, O., Pérez-Landa, G., Sanz, M.J., Scholz, Y., Facon, G., Ceschia, E., Beziat, P., 2006. The CarboEurope regional experiment strategy. Bulletin of the American Meteorological Society 87 (10), 1367–1379.

Donatelli, M., Campbell, G.S., 1998. A simple model to estimate global solar radiation. In: Proceedings of the 5th ESA Congress, pp. 133–134.

ECMWF, 2007. ERA-Interim. New ECMWF reanalysis products from 1989 onwards, ECMWF Newsletter.

EUMETSAT, 2011. MSG image data reprocessing campaign kicks off, EUMETSAT Product and Service News.

Fortin, J.G., Anctil, F., Parent, L.E., Bolinder, M.A., 2008. Comparison of empirical daily surface incoming solar radiation models. Agricultural and Forest Meteorology 148 (8–9), 1332–1340.

Garcia y Garcia, A., Guerra, L.C., Hoogenboom, G., 2008. Impact of generated solar radiation on simulated crop growth and yield. Ecological Modelling 210 (3), 312–326.

Gautier, C., Diak, G., Masse, S., 1980. A simple physical model to estimate incident solar radiation at the surface from GOES satellite data. Journal of Applied Meteorology 19 (8), 1005–1012.

Geiger, B., Meurey, C., Lajas, D., Franchisteguy, L., Carrer, D., Roujean, J.L., 2008. Near real-time provision of downwelling shortwave radiation estimates derived from satellite observations. Meteorological Applications 15 (3), 411–420.

Genovese, G.P., 1998. The methodology, the results and the evaluation of the MARS crop yield forecasting system. In: Rijks, D., Terres, J.M., Vossen, P. (Eds.), Agrometeorological Applications for Regional Crop Monitoring and Production Assessment. Office for official publications of the EU, EUR 17735 EN, Luxembourg, pp. 67–119.

Hansen, J.W., 1999. Stochastic daily solar irradiance for biological modeling applications. Agricultural and Forest Meteorology 94 (1), 53–63.

Hargreaves, G.L., Hargreaves, G.H., Riley, J.P., 1985. Irrigation water requirements for Senegal River basin. Journal of Irrigation & Drainage Engineering – ASCE 111 (3), 265–275.

Hirsch, R.M., Slack, J.R., 1984. A nonparametric trend test for seasonal data with serial dependence. Water Resources Research 20 (6), 727–732.

Hubbard, K.G., 1994. Spatial variability of daily weather variables in the high plains of the USA. Agricultural and Forest Meteorology 68 (1–2), 29–41.

Hunt, L.A., Kuchar, L., Swanton, C.J., 1998. Estimation of solar radiation for use in crop modelling. Agricultural and Forest Meteorology 91 (3–4), 293–300.

JRC, 2006. Verification of Downscaling Methods for CGMS Numerical weather based. Project deliverable under contract 22550-2004-12-F1SC-ISP-NL, Joint Research Centre, Ispra.

LandSAF, 2008. VALIDATION REPORT DSSF, SAF for Land Surface Analysis (LSA-SAF).

LandSAF, 2010. Product User Manual, Down-welling Shortwave Flux (DSSF).

Podestá, G.P., Núñez, L., Villanueva, C.A., Skansi, M.A., 2004. Estimating daily solar radiation in the Argentine Pampas. Agricultural and Forest Meteorology 123 (1–2), 41–53.

Posselt, R., Müller, R., Trentmann, J., Stöckli, R., 2010. Surface radiation climatology derived from Meteosat First and Second Generation satellites, European Geophysical Union. Geophysical Research Abstracts, Vienna.

Prescott, J.A., 1940. Evaporation from a water surface in relation to solar radiation. Transactions of the Royal Society of South Australia 64, 114–125.

Rigollier, C., Lefèvre, M., Wald, L., 2004. The method Heliosat-2 for deriving short-wave solar radiation from satellite images. Solar Energy 77 (2), 159–169.

Schulze-Kegel, D., Heidt, F.D., 1996. Mapping of global radiation with meteosat. Solar Energy 58 (1–3), 77–90.

Supit, I., 1994. Global Radiation, EUR 15745 EN. Office for Official Publications of the European Communities, Luxembourg, 200 pp.

Supit, I., van Diepen, C.A., Boogaard, H.L., Ludwig, F., Baruth, B., 2010a. Trend analysis of the water requirements, consumption and deficit of field crops in Europe. Agricultural and Forest Meteorology 150 (1), 77–88.

Supit, I., van Diepen, C.A., de Wit, A.J.W., Kabat, P., Baruth, B., Ludwig, F., 2010b. Recent changes in the climatic yield potential of various crops in Europe. Agricultural Systems 103 (9), 683–694.

Supit, I., Van Kappel, R.R., 1998. A simple method to estimate global radiation. Solar Energy 63 (3), 147–160.

Szczypta, C., Calvet, J.C., Albergel, C., Balsamo, G., Boussetta, S., Carrer, D., Lafont, S., Meurey, C., 2011. Verification of the new ECMWF ERA-Interim reanalysis over France. Hydrology and Earth System Sciences 15 (2), 647–666.

Tarpley, J.D., 1979. Estimating incident solar radiation at the surface from geostationary satellite data. Journal of Applied Meteorology 18 (9), 1172–1181.

Trigo, I.F., Dacamara, C.C., Viterbo, P., Roujean, J.L., Olesen, F., Barroso, C., Camacho-De-Coca, F., Carrer, D., Freitas, S.C., García-Haroj, J., Geiger, B., Gellens-Meulenberghs, F., Ghilain, N., Meliá, J., Pessanha, L., Siljamo, N., Arboleda, A., 2011. The satellite application facility for land surface analysis. International Journal of Remote Sensing 32 (10), 2725–2744.

Trnka, M., Žalud, Z., Eitzinger, J., Dubrovský, M., 2005. Global solar radiation in Central European lowlands estimated by various empirical formulae. Agricultural and Forest Meteorology 131 (1–2), 54–76.

van der Voet, P., van Diepen, C.A., Oude Voshaar, J., 1994. Spatial Interpolation of daily meteorological data: a knowledge based procedure for the regions of the European Community. SC report 53/3, DLO Winand Staring Centre, Wageningen.

Vossen, P., Rijks, D., 1995. Early crop yield assessment of the E.U. countries: the system implemented by the Joint Research Centre. EUR 16318, Publication of the Office for Offical Publications of the E.C., Luxembourg.